**Aquacultural Engineering**
January 2014, Volume 58, Pages 77–87
http://dx.doi.org/10.1016/j.aquaeng.2013.11.002




# C/N ratio-induced structural shift of bacterial communities inside lab-scale aquaculture biofilters

Luigi Michaud[a, *], Angelina Lo Giudice[a], Filippo Interdonato[a], Sebastien Triplet[b], Liu Ying[c], Jean Paul Blancheton[b]

[a] Dept. of Biological and Environmental Sciences, Viale F. Stagno d'Alcontres 31, University of Messina, 98166 Messina, Italy
[b] IFREMER Palavas-les-Flots, Chemin de Maguelone 34250 Palavas-les Flots, France
[c] Institute of Oceanology, Chinese Academy of Sciences, Qingdao 266071, China

*: Corresponding author : Luigi Michaud, Tel.: +0039 090 6765533 ; fax: +0039 090 6765526 ;
email address : lmichaud@unime.it

**Abstract:**

In Recirculating Aquaculture Systems (RAS) various chemical compounds (mainly nitrates and organic carbon) accumulate in the rearing water. These chemical substrata regulate the ecophysiology of the bacterial communities of the biofilter and have an impact on its nitrification efficiency and reliability.

In the present study chemical and microbiological parameters in static mineral bed (SBB) and moving plastic bed (MBB) biological filters were monitored at increasing C/N ratios ranging from 0 (pure nitrification) to 4 (combined nitrification and organic carbon removal), with the aim to investigate the shift of the bacterial community structure and major taxa relative abundances.

Results suggest that the MBB are less subjected to the nitrification reduction than the SBB, probably due to their self-cleaning characteristic. Moreover, the dynamics and flexibility of the bacterial community to adapt to influent water changes seemed to be linked with the biofilter performance. The increase of the C/N ratio resulted in a shift of the bacterial community structure in term of reduction of taxa richness and diversity indices, and in a positive selection of the Gammaproteobacteria (especially in the SBB).

One of the key aspects for improving the reliability and sustainability of RASs is a proper management of the biofilter bacterial populations, which is directly linked to the C availability. Nevertheless, it is a pertinent question whether it is possible to modify the composition of a microbial community in an environment like a biological filter, using direct microbe controlling systems (e.g. water exchange, UV disinfection, etc.).

**Highlights**

► We study the bacterial community in both mineral static bed and moving plastic bed lab-scale biological filters. ► We use five C/N ratios (from 0 to 4) to monitor nitrification efficiency and microbial community structure. ► Static bed resulted less subjected to the nitrification reduction than the static ones. ► The C/N ratio influenced the community structure in term of reduction of richness and diversity. ► One of the key aspects for the reliability of RASs is a proper management of the biofilter bacterial populations.

**Keywords :** Recirculating aquaculture system ; Biofilters ; C/N ratio ; Microbial community structure

## 1. Introduction

Recirculating aquaculture systems (RASs) employ various strategies in order to purify and reuse rearing water, thus dramatically reducing its make up water consumption compared to traditional systems. RAS technology provides the option of rearing fish at high densities under controlled conditions, leading to a potentially reduced environmental impact from the fish production (Piedrahita, 2003; Badiola et al., 2012). The understanding of the system is one of the key factors in the management of RASs, as this requires interaction between engineering and organism biology and husbandry. All the key biological mechanisms involved in the functioning of RAS therefore need to be understood and mastered. This is particularly the case processes determining the development of bacterial populations and their interactions with fish (Blancheton et al., 2013).

The efficient removal of TAN and nitrites are essential issues in relation to the commercial fish production. TAN is oxidized to nitrate in biofilters by nitrifying bacteria attached to a solid inert support medium, internally in pore spaces or directly on the surface, forming a fixed biofilm (Michaud et al., 2006; 2009; Prehn et al., 2012).

The C/N (organic carbon / inorganic nitrogen) ratio has often been used as a link between the availability and competition for organic carbon mainly composed by fish faeces and uneaten feed, and ammonium (Hu et al., 2009). At high C/N ratios the heterotrophic bacteria reduce the diffusion of nitrogenous substrate and DO to the autotrophic nitrifying bacteria, thus negatively affecting the nitrification rate (Nogueira et al., 2002; Chen et al., 2006). Reduction in TAN removal rates as high as 70% has been reported at C/N ratios above 1 for dissolved carbon (Zhu and Chen, 2001; Ling and Chen, 2005), while a reduction of 73% has been reported at a C/N ratio of 2 for particulate carbon (Michaud et al., 2006). Improved feed quality and assimilation, in addition to a better removal or finer

mechanical filtration of waste solids, are the two primary means of reducing particulate and dissolved organic concentrations in recirculating systems (Guerdat et al., 2011). Fast growing bacteria (r-strategists) are the first to exploit an increase in substrate supply but, if the resources are consumed, they can be gradually outcompeted by slower growing specialists (K-strategists)(Hansen and Olafsen, 1999).

The effect of organic carbon on biofilters has been mainly studied with respect to either the nitrifying reactor performance or the microbial spatial and quantitative distributions (Ohashi et al., 1995; FDZ-Polanco et al., 2000). The present study was aimed at investigating the effect of increasing C/N ratios on the bacterial community structure and major taxa relative abundances in aquaculture lab-scale biofilters. In particular, two biofilter configurations (mineral static bed and plastic moving bed) were tested.

## 2. Material and Methods

### *2.1. Experimental system and procedures*

#### *2.1.1. Lab-scale biofilter system*

The system was constituted by four 9.5 liter biofilters that were continuously filled with heated (20± 2°C), sand-filtered and UV disinfected seawater (salinity 37 ± 1, pH 7.5 ± 0.5) (Fig. 1). Two biofilters (replicates) were submerged reactors (defined as Static Bed Biofilter, SBB) and filled with 8 liters of a mineral packing media (cooked clay with a high specific surface usable by bacteria of about 800 $m^2/m^3$, Biogrog, Argiles et Mineraux, Montguyon, France). The other two biofilters (replicates) were set up as moving bed reactors (defined as Moving Bed Biofilter, MBB) and 2/3 filled with a plastic packing media (Acui T, specific surface of 800 $m^2/m^3$, Nantes, France).

The system was equipped with a 300 L tank for the enrichment mixture (inorganic N and organic C, as described below) and with a 1 $m^3$ tank used as a buffer for the make-up water. The raw seawater was pumped into each biofilter at a constant flow rate of 2 L/min and the concentrated enrichment mixture was pumped at a constant flow rate of 0.2 L/min. The effluent was not re-injected in the buffer thank in order to keep constant the inlet water composition.

*2.1.2. Experimental procedures*

Inlet water was enriched with particulate organic matter (POM) and ammonium chloride (see below). Theoretical C/N levels were fixed to 0, 0.5, 0.8, 2 and 4. Each C/N ratio step was set up in duplicate (two filters for MBB and two for SBB) and run for at least four weeks to allow the formation of a steady–state biofilm. Chemical and physical parameters (pH, oxygen concentration, temperature, redox potential) were daily measured.

At the end of each C/N ratio step, samples were collected for chemical and microbiological analyses (see below), and the system was subsequently set up and run again for 4 more weeks.

*2.1.3. Enrichment mixture*

The input of ammonium chloride (Sigma, France) was set to achieve an ammonia concentration of 2 mg/L at the inlet of each biofilter. This concentration was kept constant for all the experiment and the C/N ratio was modified through the change of the carbon concentration.

The organic carbon used for the experiment was composed by fish feces and unconsumed feed collected from particle separators at the outlet of various experimental seabass rearing

systems. Such mixture (94 ± 0.1% dry matter) was sterilized by autoclaving, freeze-dried and grinded in a fine homogenous powder as described in Michaud et al. (2006). The resulting powder was chemically analyzed with an auto-analyzer Carlo Erba Instruments 1500 CHN for determination of the average carbon content (42 ± 0.8% of total organic carbon, data not shown), and stored at -20°C during the entire experiment.

### *2.2. Chemical analyses*

Ammonia, nitrites and nitrates were analyzed with a Technicon® Autoanalyser II as described by Treguer and La Torre (1974). Biofilters were routinely monitored (twice a week) for TAN oxidation ($TAN_{In}$ - $TAN_{Out}$). At every sampling time, nitrification efficiency was evaluated by connecting each biofilter in batch mode and following the decreasing of the TAN in the batch for one hour. The batch mode consisted in a tank filled with 50 liters of water containing 2 mg/L of ammonia and the correct amount of POC to maintain the desired C/N ratio. Water was collected from the tank at fixed intervals (0, 20, 40 and 60 minutes).

### *2.3. Microbiological analyses*

#### *2.3.1. Sampling procedures*

Bacterial communities fixed on two Biogrog and 10 Acui-T, packing media subunits were detached following the procedure described in Michaud et al. (2006). Briefly, the packing media subunits were placed in a detachment buffer (0.1% of sodium pyrophosphate in a phosphate buffer saline, PBS: 130 mM NaCl, 10 mM $Na_2HPO_4$, and 10 mM $NaH_2PO_4$; pH 7.4), manually scraped with a sterile brush and placed in an ultrasonic iced bath for 10 min

at 20 kHz. This collected mixture was divided in aliquots for microbiological analyses. All chemicals were purchased by Sigma, France.

*2.3.2. Bacterial enumeration*

Samples for direct enumeration of free living bacteria were fixed in formalin and stored at -20°C until processing. Sample aliquots were filtered on 25 mm diameter, 0.2 µm pore size black polycarbonate filters, and stained with DAPI (4',6– diamidino–2–phenilindole, Sigma, France) (Porter and Feig, 1980). Cells were visualized by epifluorescence microscope (Axioplan, Zeiss). Results are expressed in cells/mL.

Cultivable heterotrophic bacteria associated with packing media were enumerated by Colony Forming Units (CFU/mL) on Marine Agar (2216, Difco). Plates were set up in duplicate for each dilution. Only plates with 20 to 200 colonies were considered.

*2.3.3. Fluorescent In Situ Hybridisation (FISH)*

Cell fixation was carried out with paraformaldehyde in PBS (final concentration of 4%, w/v, Sigma, France) and incubated at 4°C for 12 h (Amann et al., 1995; MacDonald and Brözel, 2000; Nogueira et al., 2002). Triplicate samples were concentrated from fixed detachment solution on white polycarbonate filters (Isopore, diameter, 25 mm; pore size, 0.2 mm). FISH was performed by using CY-3 labelled probes (MWG, M-Medical, Italy) listed in Table 1 (Meier et al., 1999; Egli et al., 2003).

Cells were observed using an Axioplan epifluorescence microscope (Zeiss) equipped with specific filter sets for DAPI and CY3. For each sample and probe, 20 fields were enumerated.

*2.3.4. DNA extraction*

For DNA extraction, 100 mL of detaching buffer for each sample were concentrated on sterile 47-mm diameter, 0.22 µm pore-size (Nuclepore) membranes and subsequently stored at -20°C until processing. DNA was extracted from the minced filters in a sterile 2 mL Eppendorf tube using the RNA/DNA extraction kit (Qiagen, Germany), following the manufacturer's instructions. The quantity and quality of DNA were checked by agarose gel electrophoresis (1%, w/v) in TAE buffer (20 mM Tris-HCl, 10 mM sodium acetate, 0.5 mM $Na_2EDTA$; pH 8.0).

*2.3.5. Denaturing Gradient Gel Electrophoresis (DGGE)*

Extracted DNA was amplified by using the eubacteria primes 1055F (5'-TGGCTGTCGTCAGCT-3') and the 1392R (5'-GTAAAACGACGGCCAG-3'), then later with a GC clamp (40 bases) at the 5' extremity.

The PCR mixture (50 µL final volume) contained both primers at 0.2 µM, 1.5 mM $MgCl_2$, 1X Buffer, 0.2 µM of every deoxynucleoside triphosphate (Fermentas, Italy) and 1.5 U of *Taq* polymerase (Bioline, Italy). The PCR cycle included an initial denaturation step consisting of 5 min at 95°C, followed by a set of seven touchdown PCR cycles (30 s of denaturation at 94°C, 30 s of annealing at 62, 60, 59, 58, 57, 56, and 55°C, and then 30 s of elongation at 72°C) and then 30 cycles of denaturation at 94°C, annealing for 30 s at 54°C, and elongation for 30 s at 72°C, with a final extension step consisting of 5 min at 72°C. Reaction products were firstly examined by using a 0.8% (w/v) agarose gel in TAE buffer and then purified with QIAquick PCR Purification kit, following the manufacturer instructions.

The DGGE was performed using a D-Code universal mutation detection system (Bio-Rad,

Richmond, CA, USA). Triplicate PCR products were combined (300 ng) and resolved on 6% (w/v) polyacrylamide (acrylamide: N,N-methylenebisacrylamide, 37.5:1) gels that contained a 40–60% denaturant gradient (100% denaturant contains 7 M urea and 40% formamide) for 20 h at 60°C and a constant voltage of 50V. Gels were stained with SYBR-Gold (1:10,000 dilution; Molecular Bio- Probes, Eugene, USA) for 30 min in the dark and then observed using a UV GelDoc apparatus (BioRad).

Gel sections containing fragments of interest were excised, placed in 50 mM Tris-HCl (pH 8.0)–1 mM $Na_2EDTA$, and incubated at 4°C overnight. The eluted DNA was used as a template for the PCR by using the same primers (without GC clamp) and in the same conditions as described above. PCR results were checked as described above, quantified by comparing the amplicon intensity with a standard (1Kb Ladder, Fermentas) and subsequently sent to an external sequencing service (BMR genomic, Italy).

Obtained sequences were compared to 16S rRNA gene sequences in the NCBI GenBank and the EMBL databases using BLAST, and the “Seqmatch” and “Classifier” programs of the Ribosomal Database Project II http://rdp.cme.msu.edu/). Phylogenetic tree (Neighbour-Joining method according to the model of Jukes-Cantor distances) was constructed by using the MEGA 5 (Molecular Evolutionary Genetics Analysis) software (Kumar et al., 1993) The robustness of the inferred trees was evaluated by 1000 bootstrap resamplings.

*2.3.6. Nucleotide sequence accession numbers*

The nucleotide sequences obtained in this work have been deposited in the GenBank database (accession numbers KC622273-KC622300).

213

214 *2.3.7. Automated Ribosomal Intergenic Spacer Analysis (ARISA)*

215 Extracted DNA was amplified using universal bacterial primers 16S-1392F (5'-
216 GYACACACCGCCCGT-3') and 23S-125R (5'-GGGTTBCCCCATTCRG-3'). The 23S-
217 125R primer was fluorescently labelled with the fluorochrome HEX (MWG, Biotech,
218 Germany). PCRs were performed in triplicate in 50 µL volumes by using an ABI 9600
219 thermocycler (PE, Applied Biosystems, USA) with an initial denaturation step at 94°C for 3
220 min, followed by 30 cycles of 94°C for 45 s, 55°C for 45 s, 72°C for 90 s, with a final
221 extension at 72°C for 5 min.

222 DNA (100 ng) was purified with QIAquik PCR purification kit (QIAGEN, Germany)
223 following manufacturer instructions and sent to an external sequencing service (BMR
224 Genomics, Italy) in order to be resolved by capillary electrophoresis on an ABI PRISM
225 3130 Analyzer (PE, Applied Biosystems, USA) with the internal size standard ROX 2500
226 (Applied Biosystems) by using the local southern size-calling method of the software
227 GeneScan 3.7 (PE, Applied Biosystems, USA).

228 To align ARISA profiles of different runs, we binned the peaks in different fixed windows
229 depending on the fragment length. All peaks smaller than 350 bp or longer than 1300 bp
230 size were not considered because the amplified fragments are composed by the ITS region
231 plus 300–350 bp belonging to the next genes (about 200 bp from 16S rRNA gene and 125
232 bp from 23S rRNA gene) (Caravati et al., 2010). The detection threshold applied to ARISA
233 profiles was calculated according to the approach suggested by Luna et al. (2006). For each
234 sample two independent ARISA reactions were run and only peaks shared by both
235 replicates were considered.

236

*2.3.8. Community Level Physiological Profile (CLPP)*

The community-level physiological profiles (CLPPs) of potential substrate used by the bacterial populations were determined with Biolog-EcoPlates™ (Hayward CA, USA) (original type) 96-well microtiter plates (Garland, 1997). The 31 substrates situated on microtiter plates were divided into five main groups (guilds): carbohydrates (*Carb*), polymers (*Poly*), carboxylic and acetic acids (*C&AA*), amino acids (*AA*), amines and amides (*A&A*), as reported by Frąc et al. (2012).

The study of bacterial populations associated to the biofilter Packing Media, microplates were inoculated with 150 µL of the same cell suspension (in detaching buffer), used for DAPI counts (before formalin fixation), and kept at room temperature (25 ± 1°C). For the determination of the physiological profile of rearing water bacteria, an aliquot of each sample was concentrated by centrifugation at 10,000 rpm at R.T. Suspensions were pre-incubated overnight in order to allow microbial utilization of any soluble organic carbon derived from the Packing Media that could interfere in the sole-C-source-use response.

For each sample Biolog plates were followed for one week by daily determination of the optical density (OD), using an automatic microplate reader at 595 nm ($OD_{595}$), and data were electronically recorded.

Microbial response in each microplate that expressed average well-colour development (AWCD) was determined as described in (Gomez et al., 2004).

***2.4. Statistical analyses***

Results of bacterial abundances were analyzed using variance analysis (one-way ANOVA). Comparison between groups for a significant difference of mean or rank values was performed after normality and variance tests.

Statistical calculations were performed with SigmaStat software for Windows, version 2.0 (Copyright 1992-1995 Jandel Corporation).

The DGGE analysis is based on the amplification of the highly conserved 16S rRNA gene, while the ARISA focuses on heterogeneous genome structures. The estimation of the bacterial community structure refers to the number of different "phylotypes" (for DGGE analyses) and "genotypes" (for ARISA) (Danovaro et al., 2006).

DGGE band patterns, ARISA peak profiles, FISH and CLPP data were analyzed (Bray–Curtis similarity) after *ad hoc* data pretreatment and arranged into a non-metric multi-dimensional scaling (nMDS) and a cluster plot by using Primer 6 software, version 6β R6 (Copyright 2004, PRIMER-E Ltd). The ordination results in a Euclidean plane in which highly similar samples are plotted close together.

To test differences in community composition and metabolic features, analysis of similarities (ANOSIM, based on Bray-Curtis similarity) was carried out. ANOSIM result produces a sample statistic, Global R-value, which represents the degree of separation between test groups (Clarke, 1993). A value close to 1 indicates that the community composition is totally different, whereas a value of 0 indicates no difference.

Similarity of percentages ("SIMPER") was used to identify species (i.e. in our case ARISA peaks, Taxa and Carbon sources) that could potentially discriminate between treatments.

## 3. Results

### *3.1. Chemical analyses*

#### *3.1.1. Nitrifying activity of biofilters*

In the SBB the ammonium oxidation rate decreased as the C/N ratio increased (Fig. 2A). $NH_4^+$-N oxidization was almost completed in 1 h at the C/N ratio 0 (95% of the initial

amount), while only 48.9% of the TAN was oxidized at the C/N ratio 4. At the three other C/N ratios 77.2 ± 2% of the TAN was oxidized. The nitrate production rate was on average 40% lower at the C/N ratios 0.5, 0.8 and 2 compared to the C/N ratio 0, while at the C/N ratio 4 it was 70% lower (not shown).

In the MBB (Fig. 2B) the TAN oxidation rate was similar at the C/N ratios from 0 to 2 (77.6 ± 4% in 1 h on average), while at C/N ratio 4 it was reduced by 59.9%. The resulting nitrate production was stable at the first four C/N ratios, while at the C/N ratio 4 it decreased on average of 30% (not shown).

### *3.2. Microbiological analyses*

#### *3.2.1. Bacterial abundances*

The viable counts in the SBB ranged from $2.09x10^4 \pm 8.43x10^3$ to $8.23x10^5 \pm 1.24x10^4$ CFU/mL at the C/N ratios 0 and 4, respectively. The total bacterial counts were between $2.53x10^6 \pm 4.23x10^5$ and $1.43x10^7 \pm 5.73x10^5$ cells/mL at the C/N ratios 0 and 4, respectively (Table 2).

Although ANOVA revealed that there was a statistically significant difference ($P<0.001$) for viable counts, the subsequent Pairwise Multiple Comparison (PMC) procedure (Tukey Test) showed no statistical significant differences between the C/N ratios 0 and 0.5, as well as between the C/N ratios 2 and 4. On the other hand, total counts were statistically different (ANOVA, $P<0.001$) and the subsequent PMC analysis confirmed such difference for all the C/N ratio pairwises, except between the C/N ratios 0 and 0.5 ($P< 0.05$). Finally, there was a linear relationship between total counts and viable counts with an $R^2$ of 0.983 ($P = 0.00275$) (not shown).

In the MBB the viable counts ranged from $3.01x10^4 \pm 8.94x10^3$ to $7.99x10^4 \pm 1.77x10^4$ CFU/mL at C/N ratios 0.5 and 0.8, respectively. The total counts ranged from $2.68x10^6 \pm 1.00x10^5$ to $3.83x10^6 \pm 1.04x10^5$ cells/mL at the C/N ratios 0 and 2, respectively (Table 2), with no statistically significant difference ($P<0.001$) among viable and total counts. However, the subsequent PMC procedure (Tukey Test) revealed that there was not a statistical significant difference among the 0, 0.5 and 0.8 C/N ratios as well as between the C/N ratios 2 and 4 ($P >0.050$) for both viable and total counts. Linear correlation showed a good $R^2$ (0.932, $P = 0.021$) between total counts and viable counts (not shown).

*3.2.2. Fluorescent in situ hybridization (FISH)*

Microbial population dynamics in biofilm packing media was firstly evaluated by using FISH with rRNA-targeted oligonucleotide probes. In addition to probes that covered most Eubacteria (EUB I-III), different specific probes were used to enumerate main bacterial groups (Table 1).

In the SBB the percentage of DAPI-stained cells enumerated by the EUB 338 probe mix ranged from 49.5 ± 7% to 79.9 ± 8% at the C/N ratios 0 and 4, respectively (ANOVA $P<0.001$) (Table 2). As it is shown in Fig. 3, FISH probes for the main phylogenetic groups, reported as percentage of EUB-stained cells, revealed that the *Gammaproteobacteria* were predominant (21.0 and 21.1%, respectively) at the C/N ratios 0 and 0.5, followed by *Alphaproteobacteria* (21 and 22%, respectively) and HGC (11 and 15.6%, respectively). At higher C/N ratios (namely 2 and 4), the *Gammaproteobacteria* (25.0 and 28.1%, respectively) and HGC (21.1 and 25.1%, respectively) became dominant,

330 whereas the *Alphaproteobacteria* remained unchanged. At C/N ratios of 2 and 4 the
331 *Betaproteobacteria* were not detected.
332 At the C/N ratio 4 an increased relative percentage of the CFB group of *Bacteroidetes* was
333 observed (21.5%). The LGC remained stable, ranging from 7 to 10.1% at the C/N ratios 0
334 and 2, respectively. Finally, the *Planctomycetes* were detected only at higher C/N ratios
335 (from 0.8 to 4), ranging from 0.2 to 2.1% (Fig. 3).
336 The subsequent SIMPER analysis pointed out that the *Gamma*- and *Alphaproteobacteria*
337 contributed for 27.3 and 26.3%, respectively, to the group similarity.
338 With regard to the MBB, the percentage of DAPI-stained cells detected by the EUB338
339 probe mix ranged from 64.4 ± 9% to 86.5 ± 10% at the C/N ratios 0.5 and 4, respectively
340 (Table 2). The Fig. 3 shows the percentage of EUB stained cells obtained for MBB by the
341 utilization of FISH probes targeting main phylogenetic groups. In this case the
342 *Gammaproteobacteria* dominated the community at each C/N ratio (ranging from 20 to
343 28.1% at the C/N ratios 0 and 4, respectively). The *Alphaproteobacteria* and CFB group of
344 *Bacteroidetes* remained stable at all C/N ratios (16.8 ± 1.3% and 15.6 ± 2.3%,
345 respectively). The LGC were maximal at the C/N ratio 0.8 (21%), whereas the HGC
346 decreased at increasing C/N ratios (ranging from 12 to 8.7%). In this case, the *Gamma*- and
347 *Alphaproteobacteria* contributed for the 28.6 and 20.9%, respectively, to the similarity of
348 MBB group (SIMPER analysis).
349 The nMDS computed on the whole FISH data-set (SBB and MBB together) revealed that
350 the community structure of the two biofilters were different in terms of relative abundance
351 of phyla (Fig. 4A).
352 On the basis of the Bray-Curtis similarities ANOSIM was computed by using the “Biofilter
353 Configuration” as factor. In our case the analysis showed a clear global difference among

354 the two biofilter configurations (R= 0.78, $p < 0.01$). Finally, SIMPER analysis pointed out
355 that between SBB and MBB the main contribution to their average dissimilarity (21.5%)
356 was due to the HGC, *Betaproteobacteria* and LGC (cumulative contribution 60.6%).
357
358 *3.2.3. Denaturating gradient gel electrophoresis analysis (DGGE)*
359 The diversity of the phylogenetic assignment of main taxa that occurred in the biofilter
360 microbiota colonizing the mineral and plastic packing media was examined by DGGE
361 analysis.
362 With regard to the SBB, the DGGE profiles obtained (not shown) for the five treatments
363 were highly reproducible. In order to obtain phylogenetic information the excised DGGE
364 gel bands were sequenced (Fig. 5). A total of 22 different bands were detected in the gel
365 and the number of DGGE bands per sample varied from 19 ± 2 to 10 ± 1 at the C/N ratios 0
366 and 4, respectively. The sequence homology between the DGGE bands and sequences
367 retrieved from the database was mainly in the range 97-100%. Six bands (namely bands 11,
368 12, 18, 19, 24 and 25) were found at all the C/N ratios. They were assigned to
369 *Pseudomonas stutzeri* (AN **KC622275**), uncultured *Nitrospirae* bacterium (AN
370 **KC622276**), uncultured bacterium clone Ba36 (AN **KC622282**), uncultured planctomycete
371 clone Cobs2TisB10 (AN **KC622283**), uncultured bacterium clone 8D-1 (AN **KC622288**)
372 and uncultured bacterium clone SWB588 (AN **KC622289**), respectively. The bands 26, 27
373 and 29, which were assigned to *Marivirga* sp. (among the CFB group of *Bacteroidetes*; AN
374 **KC622290**), uncultured *Verrucomicrobia* bacterium YNPRH34A (AN **KC622291**) and
375 uncultured betaproteobacterium clone p660 (AN **KC622293**) respectively, were detected
376 only at the C/N ratios 0 and 0.5. The band 10, namely *Roseobacter* sp. Do-34 (AN

377 **KC622274**) was retrieved at C/N ratios from 0 to 0.8. The remaining bands were spread
378 into different C/N ratios without an evident trend.
379 For the MBB 26 bands were identified with six of them (namely bands 8, 9, 13, 14, 15 and
380 24) found at all the tested C/N ratios. Among these bands, the band 8 could be ascribed to
381 *Phaeobacter* sp. (AN **KC622299**), while the other five remained unidentified, being closely
382 related to uncultured bacteria (Fig. 5). Bands 10 (*Roseobacter* sp., AN **KC622274**), 11
383 (*Pseudomonas stutzeri*, AN **KC622275**), 28 (*Mesorhizobium* sp., AN **KC622292**), as well
384 as the bands 7, 16, 22, 27, and 29 (all uncultured bacteria) were retrieved only at lower C/N
385 ratios (i.e., 0 to 0.8).
386 The bands 12 (uncultured *Nitrospirae*) and 26 (*Marivirga* sp.) were only retrieved in the
387 SBB and the bands 1, 7, 16, 21, 22 and 28 were detected only in the MBB. With the
388 exception of the band 28 (*Mesorhizobium* sp.), all these bands were ascribed to uncultured
389 bacteria. In addition the SIMPER analysis pointed out an average dissimilarity between
390 SBB and MBB of 42.74%, mainly due to the bands 12, 18, 21, 14 and 11 which were
391 cumulatively responsible for the 25.38% of group dissimilarity.
392 DGGE band patterns (presence/absence) were used to compute an nMDS (Fig. 4B). The
393 difference between the two biofilter configurations was low, at least for the lowest C/N
394 ratios (i.e., 0 and 0.5). This was confirmed by the ANOSIM analysis (Global R of 0.374, P<
395 0.01).
396
397 *3.2.4. Automated ribosomal intergenic spacer analysis (ARISA)*
398 The genetic structure of the biofilter bacterial communities was characterised by using the
399 automated ribosomal intergenic spacer analysis (ARISA) DNA fingerprint. This approach
400 was selected as it allows a rapid examination of the structure of bacterial communities and

401 because it was demonstrated to be sensitive and robust to detect changes in complex
402 communities.
403 With regard to the SBB, fragments of between 300 and 1,300 bp were resolved by the
404 ARISA technique and the community fingerprints were quite different among the different
405 C/N ratios. Richness ranged from 77 ± 6 to 53 ± 1 taxa (genotypes or ARISA fragments) at
406 the C/N ratios 0 and 4, respectively. Only 12 taxa were common to all the C/N ratios, while
407 29 fragments were found exclusively at the C/N ratio 0.
408 Similarly, for the MBB the genotype richness ranged from 71 ± 1 to 49 ± 3 at the C/N
409 ratios 0 and 4, respectively. Nine taxa were common to all the C/N ratios, whereas 17 and
410 16 taxa were exclusive of the C/N ratios 0 and 0.5, respectively.
411 The nMDS computed on the ARISA fragments pointed out that the two biofilter
412 configurations were different in their community genetic structure at all the C/N ratios, with
413 the exception of the C/N ratio 0 (Fig. 4C). In particular, the carbon load effect seems to be
414 more evident for the SBB than for MBB. The formers are spread in a larger group on the
415 nMDS plot. The ANOSIM test (on Bray-Curtis similarities), also computed by using the
416 "Biofilter Configuration" as factor, suggested a genetic difference among the two biofilter
417 communities ($R = 0.553$ $p < 0.02$). The SIMPER analysis pointed out that the main
418 contribution to their average dissimilarity (63.56%) between SBB and MBB was due to 83
419 fragments out of 197 totally detected (for a cumulative contribution of 63.56%).
420
421 *3.2.5. Community level physiological profile (CLPP)*
422 In the SBB the number of oxidized substrata increased from 23 (74.2%) at C/N 0 to 25
423 (80.65%) at C/N 0.5, and to 29 (93.5%) at the three remaining C/N ratios (namely 0.8, 2
424 and 4) (Fig. 6). In particular, the oxidation of carbohydrates (*Carb* guild) increased at

425 increasing C/N ratios, ranging from 70 and 80% at the C/N ratios 0 and 0.5, respectively, to
426 90 % at the highest C/N. At each C/N ratio (except for the C/N ratio 0) all the polymers
427 (*Poly*), namely alpha-cyclodextrin, glycogen, tween 40 and tween 80 were oxidized. On
428 average the 90% of the carboxylic and acetic acids (*C&AA* guild) were oxidized. The guild
429 aminoacids (*AA*) was oxidized at 50 and 67% at the C/N ratios 0 and 0.5, respectively,
430 while all the AA substrata were oxidized at the higher C/N ratios. Finally, the two
431 amines/amides (*A&A* guild) were always used (namely phenylethyl-amine and putrescine).
432 For the MBB the oxidized substrata ranged from 20 (64.52%) to 23 (74.2 %) at the C/N
433 ratios 0 and 0.8, respectively (Fig. 6). Any guild was not entirely oxidized at all the C/N
434 ratios. The oxidation of *Carb* guild shifted from 70% at the C/N ratio 0 to 80% at the C/N
435 ratios of 0.5 and 0.8 and, finally, returned to 70% at the higher C/N ratios. The polymer
436 guild (*Poly*) was oxidized at 75% at the C/N ratios 0 and 0.5, and at 50% at the other C/N
437 ratios, with tween 40 that was never oxidized and tween 80 that was not used at higher C/N
438 ratios. All but one (2-hydroxy benzoic acid) carboxylic and acetic acids (*C&AA* guild) were
439 used at the C/N ratio 0. At the other C/N ratios the 2-hydroxy benzoic, gamma-
440 hydroxybutyric and itaconic acids were never used. The oxidation of the aminoacid guild
441 (*AA*) increased from 33% at the C/N ratio 0 (with only the L-asparagine and L-serine that
442 were oxidized) to 50% at the C/N 0.5 and to 83% at the remaining C/N ratios. L-thronine
443 was never used. The two amines/amides (*A&A* guild) were not oxidized at the C/N ratios 0
444 and 0.5.
445 The rate of substrate utilization (catabolic potential) was used to compute a multivariate
446 analysis. The nMDS ordination of the CLPP data-set confirmed that the two biofilter
447 configurations were different in terms of their microbial community functional diversity.
448 This was stressed by the ANOSIM result of 0.648 (global R, $p < 0.01$).

449 The SIMPER analysis pointed out that between SBB and MBB, the main contribution to
450 their average dissimilarity (36%) was due to 12 (up to 31) substrata, representing a
451 cumulative contribution of 50.44%: pyruvic acid methyl ester, beta-methyl-D-glucoside, N-
452 acetyl-D-glucosamine, D,L-alpha-glycerol-phosphate (*Carb* guild); glycogen, alpha-
453 cyclodextrin, tween 40, tween 80 (*Poly* guild); D-galactonic acid lactone and D-
454 glucosaminic acid (*C&AA* guild); L-threonine and L-asparagine (*AA* guild) .
455

456 **4. Discussion**

457 The accumulation of biodegradable organic carbon in the rearing water of aquaculture
458 systems supports the heterotrophic activity and allows the establishment of competition
459 mechanisms for oxygen, nutrients and space between chemoautotrophic nitrifiers and
460 heterotrophs, causing a reduction of the nitrification rates (Zhu and Chen, 2001; Michaud et
461 al., 2006).
462 In the present study, chemical and microbiological parameters in static mineral bed and
463 moving plastic bed biological filters were monitored at increasing C/N ratios ranging from
464 0 (pure nitrification) to 4 (combined nitrification and organic carbon removal). The TAN
465 removal efficiency was reduced by 50 and 40% at increasing C/N ratios in SBB and MBB,
466 respectively. This effect has been widely documented (Zhu and Chen, 2001; Ling and
467 Chen, 2005; Michaud et al., 2006), but the nitrification efficiency reduction varies from
468 experiment to experiment based on several parameters such as biofilter type and scale, feed
469 composition and loads.
470 Our data suggest that the MBB are less subjected to the nitrification reduction than the
471 SBB. This could be due to the self-cleaning characteristic of the moving bed plastic media.

In turn, the mineral Biogrog acts as a mechanical filter, trapping huge amount of particulate matter (Franco-Nava et al., 2004).

Ling and Chen (2005) reported significant differences in TAN removal rates at the C/N ratio 0 for three filter types (floating bead, fluidized sand and submerged bio-cubes), but little differences between the three filter types at the C/N ratio 2, which indicated that high organic carbon loads on nitrification tend to equalize the performance characteristics between filter types. This seems not to be true for the two biofilter types tested in this work. In our experiments, an increasing C/N ratio resulted in an increase of the total and cultivable bacterial abundances, reaching values comparable with those previously reported (Blancheton et al., 2013 and references therein). In a RAS, as in every other environment, heterotrophic bacterial activity is mainly regulated by the biologically available organic carbon in the system. The supply of organic matter is typically the growth limiting factor defining the number of heterotrophic bacteria that can be sustained over time, and it was defined as carrying capacity (CC) (Attramadal et al., 2012). In our case the bacterial abundances were comparable in the two biofilter types at the first two C/N ratios. An increasing carbon load resulted in a more obvious increase of total bacteria in the SBB (one log higher than the MBB at the C/N ratios 2 and 4).

Cultivability increased only slightly in the MBB, whereas the carbon trapped in the SBB allowed increasing the cultivability up to six times. As the ability to grow quickly on a nonselective agar medium could be considered as a characteristic of opportunistic bacteria, the cultivability and percentage of cultivable cells may be an indicator of the succession of microbial populations. In highly carbon loaded environments opportunistic r-strategist bacteria, which invest a lot of energy in growth and reproduction, can easily outcompete the K-strategist ones, which are more efficient in energy maintenance at low carbon

concentrations. Vadstein and colleagues (1993) developed the concept that a microbially matured water, containing a more diverse and resilient microbial communities of K-strategist selected specialists is important to maintain a safe rearing environment. In turn a low maturity situation with a high percentage of fast-growing r-strategist bacteria is believed to be potentially detrimental. In fish on-growing RAS, maintaining a large community of stable microbial K-strategist is favoured by the slow variations of the organic carbon availability (Franco-Nava et al., 2004).

In this study a combination of FISH (at phyla or groups level), DGGE (at genus/species level) and ARISA (at species/subspecies level) techniques were applied. Moreover, a CLPP approach was used to investigate the effect of the C/N ratio increase on the microbial community physiology.

Our results show that the microbial community structure is strongly influenced by water quality and that the dynamics and flexibility of the bacterial community to adapt to influent water changes can be linked with the biofilter performance. The nMDS plots showed a general trend where communities of the two biofilter types are completely different regardless to the influence of C/N ratio. The different support material (mineral or plastic) support the growth of different bacterial taxa. In particular, all the three techniques, namely FISH, DGGE and ARISA, confirmed differences between SBB and MBB communities.

At increasing C/N ratios, FISH results put on evidence a positive selection for the *Gammaproteobacteria*. Many members in this group are reported to be typically copiotrophs, adapted to high nutrient concentrations. In turn, the relative percentage of the *Alphaproteobacteria* remained stable at the tested C/N ratios for both biofilter types, confirming the widespread occurrence of members in marine environments. The lack of *Betaproteobacteria* signal, which include the autotrophic nitrifiers *Nitrosomonas* spp. and

520 *Nitrosospira* spp., in SBB at C/N 2 and 4, could explain the reduction of nitrification
521 efficiency in these filters.
522 The *Planctomycetes* are typical and widespread in marine ecosystems, often found
523 associated with marine macroaggregates (Tal et al., 2006).
524 The bacterial community structure of the biofilters, determined by DGGE, with the *Alpha-*
525 and *Gammaproteobacteria*, CFB group of *Bacteroidetes* and *Planctomycetales* is generally
526 reported as the most abundant phylotypes in marine environments. In particular, ten
527 sequenced bands up to 28 belonged to the *Alpha-* and *Gammaproteobacteria*. The former
528 were mainly represented by *Hyphomicrobium* sp. (filamentous bacteria that are often
529 reported in both sewage treatment plants and adjacent waters) (Layton et al., 2000),
530 *Mesorhizobium* sp. (Gram-negative soil bacteria implicated in the formation of nitrogen-
531 fixing nodules on the roots and stems of leguminous plants, or causing gall disease and root
532 hair disease) (Kwon et al., 2005) and *Roseobacter* sp. (members of this genus are excellent
533 biofilm-forming organisms and among the first dominant surface colonizers in marine
534 environments). The *Gammaproteobacteria* were mainly represented by the genera *Vibrio*
535 and *Pesudomonas*. *Vibrio* spp. are widespread in marine environments, including estuaries,
536 coastal waters, and sediments. The *Vibrionaceae* include species that are opportunistic fish
537 pathogens. They are found in aquaculture settings, where conditions seem to enhance their
538 virulence (Thompson et al., 2009). Finally, *Pseudomonas stutzeri* is a dinitrogen-producing,
539 denitrifying bacterium, widely distributed in the environment. The presence of this
540 bacterium, which is also able to carry out heterotrophic nitrification and aerobic
541 denitrification (Zhang et al., 2011), could explain the discrepancies when calculating the
542 mass balance of nitrogen compounds between inlet and outlet of filters (data not shown). It
543 has been isolated as an opportunistic pathogen from humans and it has also been proposed

544 as a model organism for denitrification studies. These results are in line with those reported
545 by Tal et al. (2003) who applied a DGGE approach to a moving bed bioreactor and detected
546 ten different bacterial taxa, including the *Proteobacteria* and *Planctomycetes*.
547 The increase of the C/N ratio caused a dramatic increase in the substrata utilization in the
548 SBB (from the C/N ratio 0.8 to 4; 93.5% of substrata were oxidized), while in the MBB
549 only 71% of all substrata were used at the higher C/N ratios. This discrepancy can be due to
550 the differences in community structure/composition and/or on the fact that particulate
551 organic matter remained trapped on the mineral support of SBB where decomposition
552 mechanisms can occur. Biofilms are spatially structured communities of microbes whose
553 function is dependent on a complex web of factors. The increase of the C/N ratio resulted,
554 both for the static and moving beds, in a shift of the bacterial community structure in term
555 of reduction of taxa richness.
556 Probably, in an environment like a RAS, where the carbon load in the biofilter depends on
557 various factors (e.g. fish feed, mechanical filtration efficiency, routine management and/or
558 systems malfunction), the bacterial population colonizing biofilters tend to shift from a K-
559 strategy situation to a r-strategy one. In general, copiotroph r-strategists present specific
560 orthologous gene clusters conferring them the capacity to rapidly and tightly regulate
561 metabolism and nutrient acquisition (e.g. by activating alternative catabolic pathways) and
562 they can rapidly respond to changing environmental conditions, such as sudden nutrient
563 influx or depletion (Lauro et al., 2009). This is in line with a previous investigation
564 demonstrating that the increased C/N ratio caused an increase of the presence of
565 copiotrophic and potentially harmful vibrios (Michaud et al., 2006).
566

567 **5. Conclusions**

One of the key aspects for improving the reliability and the sustainability of RAS is a proper management of the biofilter bacterial populations. Biofilms, which are complex communities of interacting microorganisms integrating responses to chemical stressors (Schreier et al., 2010), play an important role in all aquatic ecosystems due to their pivotal position at the interface between physical–chemical and biotic components.

Nevertheless, it is a pertinent question whether it is possible to modify the composition of a microbial community in an environment like a biological filter, in which direct microbe controlling systems (e.g. water exchange, UV disinfection, etc.) are not really effective.

In this work we demonstrated that carbon concentration in rearing water not only affects the biofilter nitrification efficiency, but also the microbial community structure. This strengthens the idea that increasing the carbon removal efficiency will reduce the risk of proliferation of fast-growing r-strategist bacteria, eventually including pathogens, but surely consuming oxygen, clogging filters and releasing potentially harmful substances.

***Acknowledgement***

This work was done in the framework of the French-China project Programme de Recherche Avancée (PRA) 2007 - 2008: “Amélioration du fonctionnement des systèmes en recirculation pour réduire l’impact environemental de l’aquaculture-optimisation de la filtration biologique” and the Doctoral School ‘‘Dottorato di Ricerca in Scienze Ambientali: Ambiente Marino e Risorse’’ of the University of Messina, Italy. Authors wish to tank all the Ifremer technical staff for their enthusiastic and valuable support.

590 **References**

591 Amann, R.I., Ludwig, W., Schleifer, K.-H., 1995. Phylogenetic identification and in situ
592 detection of individual microbial cells without cultivation. Microbiological Reviews 59,
593 143-169.

594 Attramadal, K.J.K., Salvesen, I., Xue, R., Øie, G., Størseth, T.R., Vadstein, O., Olsen, Y.,
595 2012. Recirculation as a possible microbial control strategy in the production of marine
596 larvae. Aquacultural Engineering 46, 27-39.

597 Badiola, M., Mendiola, D., Bostock, J., 2012. Recirculating Aquaculture Systems (RAS)
598 analysis: main issues on management and future challenges. Aquacultural Engineering 51,
599 26-35.

600 Blancheton, J.P., Attramadal, K.J.K., Michaud, L., Roque d'Orbcastel, E., Vadstein, O.,
601 2013. Recirculation systems in Europe: state of the art and insight into bacterial
602 populations. Aquacultural Engineering 53, 30-39.

603 Caravati, E., Callieri, C., Modenutti, B., Corno, G., Balseiro, E., Bertoni, R., Michaud, L.,
604 2010. Picocyanobacterial assemblages in ultraoligotrophic Andean lakes reveal high
605 regional microdiversity. Journal of Plankton Research 32, 357-366.

606 Chen, S., Ling, J., Blancheton, J.P., 2006. Nitrification kinetics of biofilm as affected by
607 water quality factors. Aquacultural Engineering 34, 79-197.

608 Clarke, K.R., 1993. Non-parametric multivariate analyses of changes in community
609 structure. Australian Journal of Ecology 18, 117-143.

610 Danovaro, R., Luna, G.M., Dell'Anno, A., Pietrangeli, B., 2006. Comparison of two
611 fingerprinting techniques, terminal restriction fragment length polymorphism and
612 automated ribosomal intergenic spacer analysis, for determination of bacterial diversity in
613 aquatic environments. Applied and Environmental Microbiology 72, 5982-5989.

614 Egli, K., Bosshard, F., Werlen, C., Lais, P., Siegrist, H., Zehnder, A.J.B., van der Meer,
615 J.R., 2003. Microbial composition and structure of rotating biological contactor biofilm
616 treating ammonium-rich wastewater without organic carbon. Microbial Ecology 45, 419-
617 432.
618 FDZ-Polanco, F., Méndez, E., Uruena, M.A., Villaverde, S., Garcia, P.A., 2000. Spatial
619 distribution of heterotrophic and nitrifiers in a submerged biofilter for nitrification. Water
620 Research 34, 4081-4089.
621 Frąc, M., Oszust, K., Lipiec, J., 2012. Community Level Physiological Profiles (CLPP),
622 characterization and microbial activity of soil amended with dairy sewage sludge. Sensors
623 12, 3253-3268.
624 Franco-Nava, M.A., Blancheton, J.P., Deviller, G., Le-Gall, J.Y., 2004. Particulate matter
625 dynamics and transformations in recirculating aquaculture system: application of stable
626 isotope tracers in seabass rearing. Aquacultural Engineering 31, 135-155.
627 Garland, J.L., 1997. Analysis and interpretation of community-level physiological profiles
628 in microbial ecology. FEMS Microbiology Ecology 24, 289-300.
629 Gomez, E., Garland, J., Conti, M., 2004. Reproducibility in the response of soil bacterial
630 community-level physiological profiles from a land use intensification gradient. Applied
631 Soil Ecology 26, 21-30.
632 Guerdat, T.C., Losordo, T.M., Classen, J.J., Osborne, J.A., DeLong, D., 2011. Evaluating
633 the effects of organic carbon on biological filtration performance in a large scale
634 recirculating aquaculture system. Aquacultural Engineering 44, 10-18.
635 Hansen, G.H., Olafsen, J.A., 1999. Bacterial interactions in early stages of marine cold
636 water fish. Microbial Ecology 38, 1-26.

637 Hu, J., Li, D., Liu, Q., Tao, Y., He, X., Wang, X., Li, X., Gao, P., 2009. Effect of organic
638 carbon on nitrification efficiency and community composition of nitrifying biofilms.
639 Journal of Environmental Sciences 21, 387-394.
640 Kumar, S., Tamura, K., Nei, M., 1993. Mega: Molecular evolutionary genetics analysis,
641 version 1.02. The Pennsylvania State University, University Park, Pa 16802.
642 Kwon, S.W., Park, J.Y., Kim, J.S., Kang, J.W., Cho, Y.H., Lim, C.K., Parker, M.A., Lee,
643 G.B., 2005. Phylogenetic analysis of the genera *Bradyrhizobium*, *Mesorhizobium*,
644 *Rhizobium* and *Sinorhizobium* on the basis of 16S rRNA gene and internally ztranscribed
645 spacer region sequences. International Journal of Systematic and Evolutionary
646 Microbiology 55, 263-70.
647 Lauro, F.M., McDougald, D., Thomas, T., Williams, T.J., Egan, S., Rice, S., DeMaere,
648 M.Z., Ting, L., Ertan, H., Johnson, J., Ferriera, S., Lapidus, A., Anderson, I., Kyrpides, N.,
649 Munk, A.C., Detter, C., Han, C.S., Brown, M.V., Robb, F.T., Kjelleberg, S., Cavicchioli.
650 R., 2009. The genomic basis of trophic strategy in marine bacteria. PNAS 106, 15527-
651 15533.
652 Layton, A.C., Karanth, P.N., Lajoie, C.A., Meyers, A.J., Gregory, I.R., Stapleton, R.D.,
653 Taylor, D.E., Sayler, G.S., 2000. Quantification of *Hyphomicrobium* populations in
654 activated sludge from an industrial wastewater treatment system as determined by 16S
655 rRNA analysis. Applied and Environmental Microbiology 66, 1167-1174.
656 Ling, J., Chen, S.L., 2005. Impact of organic carbon on nitrification performance of
657 different biofilters. Aquacultural Engineering 33, 150-162.
658 Luna, G.M., Dell'Anno, A., Danovaro, R., 2006. DNA extraction procedure: a critical issue
659 for bacterial diversity assessment in marine sediments. Environmental Microbiololy 8, 308-
660 320.

MacDonald, R., Brözel, V.S., 2000. Community analysis of bacterial biofilms in a simulated recirculating cooling–water systems by fluorescent in situ hybridization with rRNA–targeted oligonucleotide probes. Water Research 34, 2439-2446.

Manz, W., Amann, R., Ludwig, W., Vancanneyt, M., Schleifer, K.-H., 1996. Application of a suite of 16S rRNA-specific oligonucleotide probes designed to investigate bacteria of the phylum Cytophaga-Flavobacter-Bacteroides in the natural environment. Microbiology 142, 1097-1106.

Meier, H., Amann, R., Ludwig, W., Schleifer, K.-H., 1999. Specific oligonucleotide probes for in situ detection of a major group of gram-positive bacteria with low DNA G+C content. Systematic and Applied Microbiology 22, 186-196.

Michaud, L., Blancheton, J.P., Bruni, V., Piedrahita, R., 2006. Effect of particulate organic carbon on heterotrophic bacterial populations and nitrification efficiency in biological filters. Aquacultural Engineering 34, 224-233.

Michaud, L., Lo Giudice, A., Troussellier, M., Smedile, F., Bruni, V., Blancheton, J.P., 2009. Phylogenetic characterization of the heterotrophic bacterial communities inhabiting a marine Recirculating Aquaculture System. Journal of Applied Microbiology 107, 1935-1946.

Neef, A., Amann, R., Schlesner, H., Schleifer, K.-H., 1998. Monitoring a widespread bacterial group: in situ detection of planctomycetes with 16S rRNA-targeted probes. Microbiology 144, 3257-3266.

Nogueira, R., Melo, L.F., Purkhold, U., Wuertz, S., Wagner, M., 2002. Nitrifying and heterotrophic population dynamics in biofilm reactor: effects of hydraulic retention time and presence of organic carbon. Water Research 36, 469-481.

684 Ohashi, A., Viraj de Silva, D.G., Mobarry, B., Manem, J.A., Stahl, D.A., Rittman, B.E.,
685 1995. Influence of substrate C/N ratio on the structure of multi-species biofilms consisting
686 of nitrifiers and heterotrophs. Water Science and Technology 32, 75-84.
687 Piedrahita, R.H., 2003. Reducing the potential environmental impact of tank aquaculture
688 effluents through intensification and recirculation. Aquaculture 226,35-44.
689 Porter, K.G., Feig, Y.S., 1980. The use of DAPI for identifying and counting aquatic
690 microflora. Limnology and Oceanography 25, 943-948.
691 Prehn, J., Waul, C.K., Pedersen, L.F., Arvin, E., 2012. Impact of water boundary layer
692 diffusion on the nitrification rate of submerged biofilter elements from a recirculating
693 aquaculture system. Water Research 46, 3516-3524.
694 Schreier, H.J., Mirzoyan, N., Saito, K., 2010. Microbial diversity of biological filters in
695 recirculating aquaculture systems. Current Opinion in Biotechnology 21, 318-325.
696 Tal, Y., Watt, J.E.M., Schreier, S.B., Sowers, K.R., Shreier, H.J., 2003. Characterization of
697 the microbial community and nitrogen transformation processes associated with moving
698 bed bioreactors in a closed recirculated mariculture system. Aquaculture 215,187-202.
699 Tal, Y., Watts, J.E.M., Schreier, H.J., 2006. Anaerobic ammonium-oxidizing (anammox)
700 bacteria and associated activity in fixed-film biofilters of a marine recirculating aquaculture
701 system. Applied and Environmental Microbiology 72, 2896-2904.
702 Thompson, C.C., Vicente, A.C.P., Souza, R.C., Vasconcelos, A.T.R., Vesth, T., Alves, N.,
703 Ussery, D.W., Iida, T., Thompson, F.L., 2009. Genomic taxonomy of vibrios. BMC
704 Evolutionary Biology 9, 258.
705 Treguer, P., La Torre, P., 1974. Manual d'analyse des sels Nutritifs dans l'eau de mer.
706 Utilisation de l'autoanaliseur II, Technicon. Universite´ de Bretagne Occidentale
707 (Publisher), Brest, France.

Vadstein, O., Øie, G., Olsen, Y., Salvesen, I., Skjermo, J., Skjak-braek, G., 1993. A strategy to obtain microbial control during larval development of marine fish, p 69-75. *In* Reinertsen, H., Dahle, L.A., Jørgensen, L., Tvinnereim, K., Balkema, A.A. (eds), Proceedings of the First international Conference on Fish Farming Technology, Rotterdam.

Zhang, J., Wu, P., Hao, B., Yu, Z. 2011. Heterotrophic nitrification and aerobic denitrification by the bacterium Pseudomonas stutzeri YZN-001. Bioresource Technology 102, 9866-9869.

Zhu, S., Chen, S., 2001. Effects of organic carbon on nitrification rate in fixed film biofilters. Aquacultural Engineering 25,1-11.

**Figure legends**

**Fig. 1 -** Schematic diagram of the Lab-scale biofilter system. 1) Static Bed Biofilters (x 2, Biogrog packing media); 2) Moving Bed Biofilters (x 2, Acui T media); 3) Flow metres (x 4); 4) sampling ports for waters analyses (x 2 for each filter); 5) sampling port for packing media; 6) Air line; 7) circulation pump; 8) peristaltic pump for nutrients enrichments; 9) enrichment reservoir; 10) water inlet; 11) water outlet.

**Fig. 2 -** Changes in $NH^{4+}$-N concentrations versus time at different C/N ratios. (a) Static Bed Biofilter and (b) Moving Bed Biofilter.

**Fig. 3 -** Percentages of EUB-stained cells detected by FISH with probes for *Proteobacteria* (*Alpha*, *Beta*, *Gamma*, *Delta* and *Epsylon*), *Cytophaga-Flavobacter* (CFB), *Actinobacteria* (HGC), *Firmicutes* (LCG) and *Planctomycetes* (Planct) at different C/N ratios. SB, Static Bed Biofilter; MB, Moving Bed Biofilter.

730 **Fig. 4 -** nMDS ordination plot comparing SBB (▲) and MBB (○) bacterial communities at
731 different C/N ratios. (a) FISH, (b) DGGE, (c) ARISA and (d) CLPP. Circles delineate
732 clusters that best separate the two biofilter communities.
733 **Fig. 5 -** Rooted phylogenetic tree calculated by Jukes-Cantor distance estimation algorithm
734 showing affiliation of DGGE bands closest-related sequences. The tree was out grouped
735 with 16S rRNA gene sequence of *Methanocaldococcus jannaschii* DSM 2661.
736 **Fig. 6 -** Percentage of total carbon source utilization at different C/N ratios for the different
737 guilds. Carbohydrates (*Carb*), polymers (*Poly*), carboxylic and acetic acids (*C&AA*), amino
738 acids (*AA*), amines and amides (*A&A*). SB, Static Bed Biofilter; MB, Moving Bed Biofilter.
739

748
749
750 **Table 2 -** Total and viable bacterial abundances, cultivability and EUB338-stained cells
751 (mean ± sd).
752

| Filter type | C/N ratio | Viable counts (CFU $ml^{-1}$) | | Total counts (cells $ml^{-1}$) | | Cultivability (%) | EUB338-stained cells (% of DAPI ) |
|---|---|---|---|---|---|---|---|
| SBB | 0 | $2.09x10^4$ | $8.43x10^3$ | $2.53x10^6$ | $4.23x10^5$ | 0.83 | 49.5 ± 7 |
| | 0.5 | $7.30x10^4$ | $2.45x10^4$ | $3.25x10^6$ | $3.33x10^4$ | 2.25 | 55.4 ± 9 |
| | 0.8 | $3.80x10^5$ | $1.09x10^5$ | $5.78x10^6$ | $6.22x10^5$ | 6.59 | 50.2 ± 5 |
| | 2 | $6.81x10^5$ | $1.30x10^5$ | $1.30x10^7$ | $2.19x10^5$ | 5.25 | 59.9 ±3 |
| | 4 | $8.23x10^5$ | $1.24x10^5$ | $1.43x10^7$ | $5.73x10^5$ | 5.75 | 79.9 ±8 |
| MBB | 0 | $3.65x10^4$ | $4.62x10^3$ | $2.68x10^6$ | $1.00x10^5$ | 1.36 | 70.3 ± 9 |
| | 0.5 | $3.01x10^4$ | $8.94x10^3$ | $2.94x10^6$ | $3.07x10^5$ | 1.02 | 64.4 ± 9 |
| | 0.8 | $5.02x10^4$ | $1.17x10^3$ | $2.93x10^6$ | $1.00x10^5$ | 1.71 | 68.1 ± 6 |
| | 2 | $7.99x10^4$ | $1.77x10^4$ | $3.83x10^6$ | $1.04x10^5$ | 2.09 | 70.1 ± 5 |
| | 4 | $7.94x10^4$ | $3.54x10^3$ | $3.62x10^6$ | $1.19x10^5$ | 2.22 | 86.5 ± 10 |

753
754
755
756

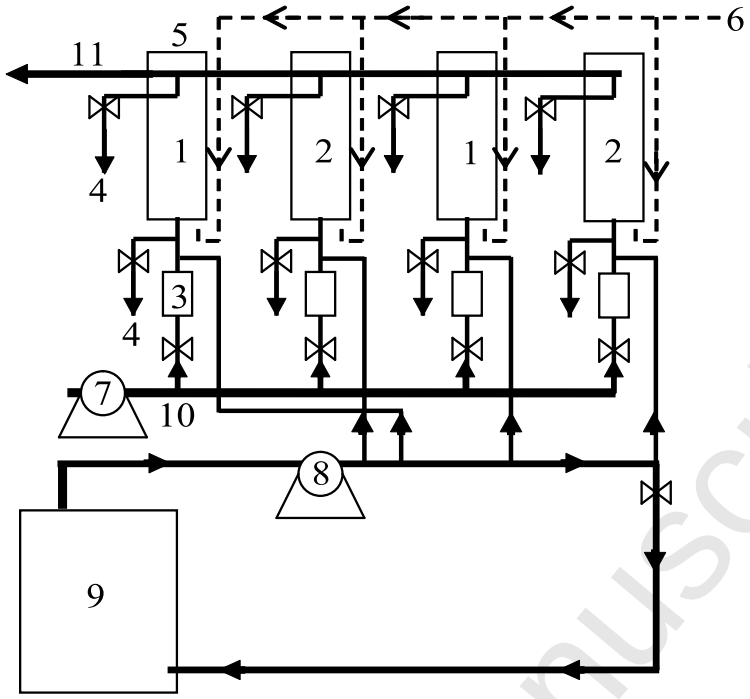


**Fig. 1 -** Schematic diagram of the Lab-scale biofilter system. 1) Static Bed Biofilters (x 2, Biogrog packing media); 2) Moving Bed Biofilters (x 2, Acui T media); 3) Flow metres (x 4); 4) sampling ports for waters analyses (x 2 for each filter); 5) sampling port for packing media; 6) Air line; 7) circulation pump; 8) peristaltic pump for nutrients enrichments; 9) enrichment reservoir; 10) water inlet; 11) water outlet.

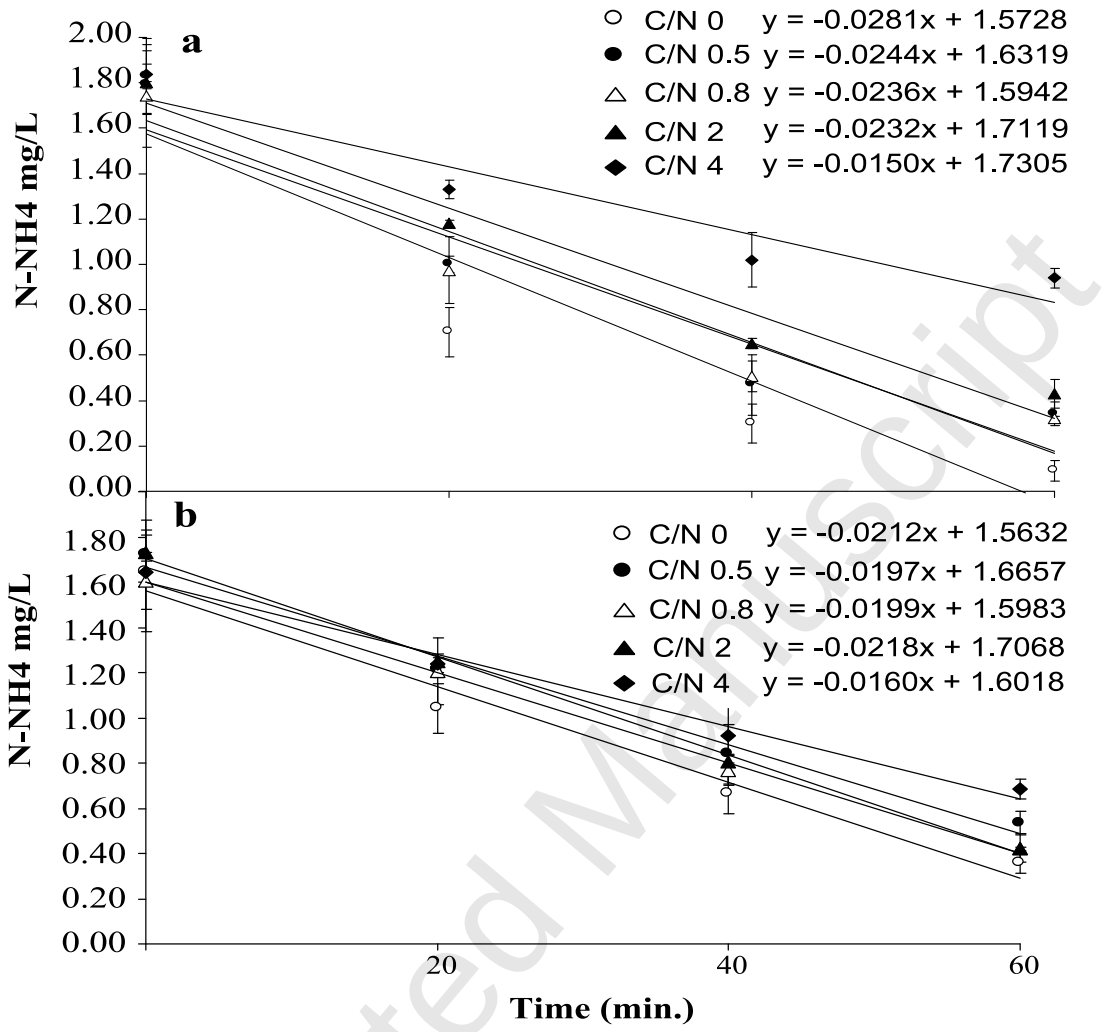


**Fig. 2 -** Changes in $NH^{4+}$-N concentrations versus time at different C/N ratios. (a) Static Bed Biofilter and (b) Moving Bed Biofilter.

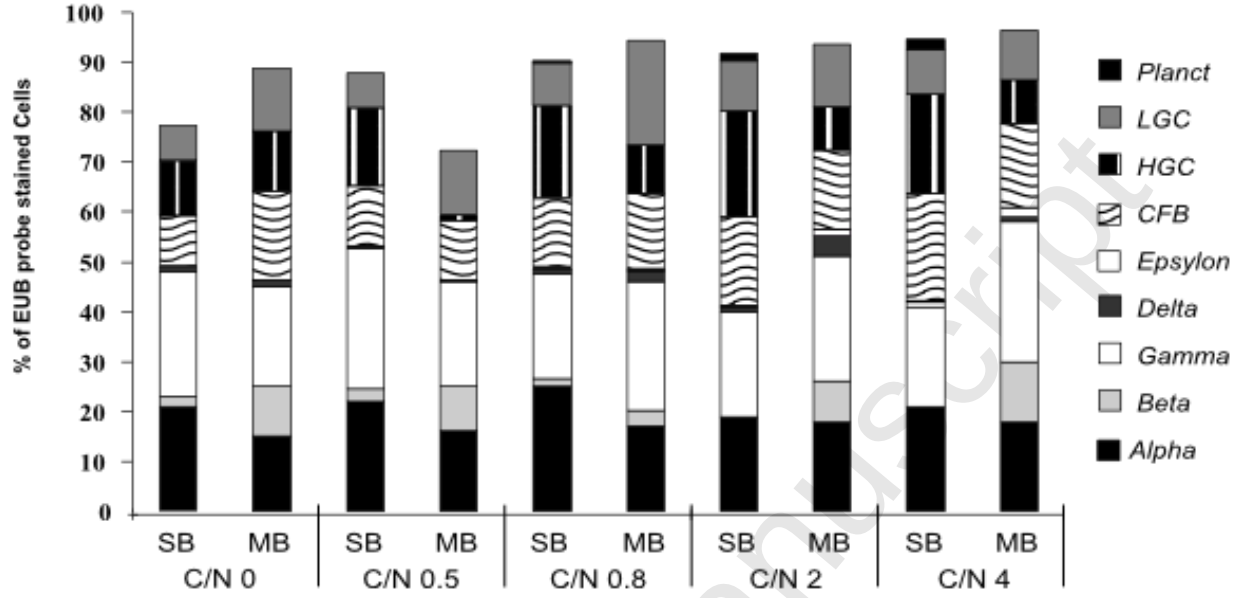


**Fig. 3 –** FISH results. Percentages of EUB-stained cells detected with probes for *Proteobacteria* (*Alpha*, *Beta*, *Gamma*, *Delta* and *Epsylon*), *Cytophaga-Flavobacter* (CFB), *Actinobacteria* (HGC), *Firmicutes* (LCG) and *Planctomycetes* (Planct) at different C/N ratios. SB, Static Bed Biofilter; MB, Moving Bed Biofilter.

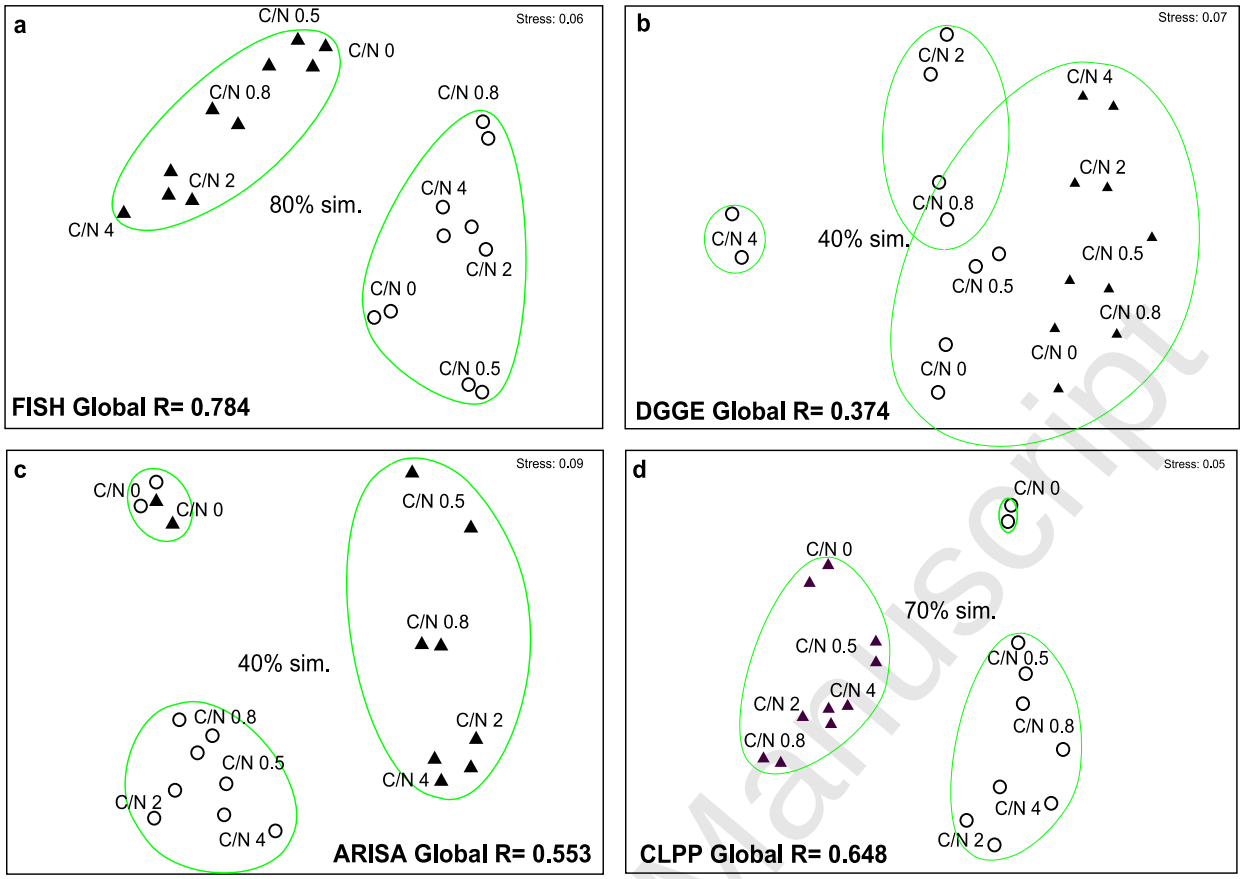


**Fig. 4 -** nMDS ordination plot comparing SBB (▲) and MBB (O) bacterial communities at different C/N ratios. (a) FISH, (b) DGGE, (c) ARISA and (d) CLPP. Circles delineate clusters that best separate the two biofilter communities.

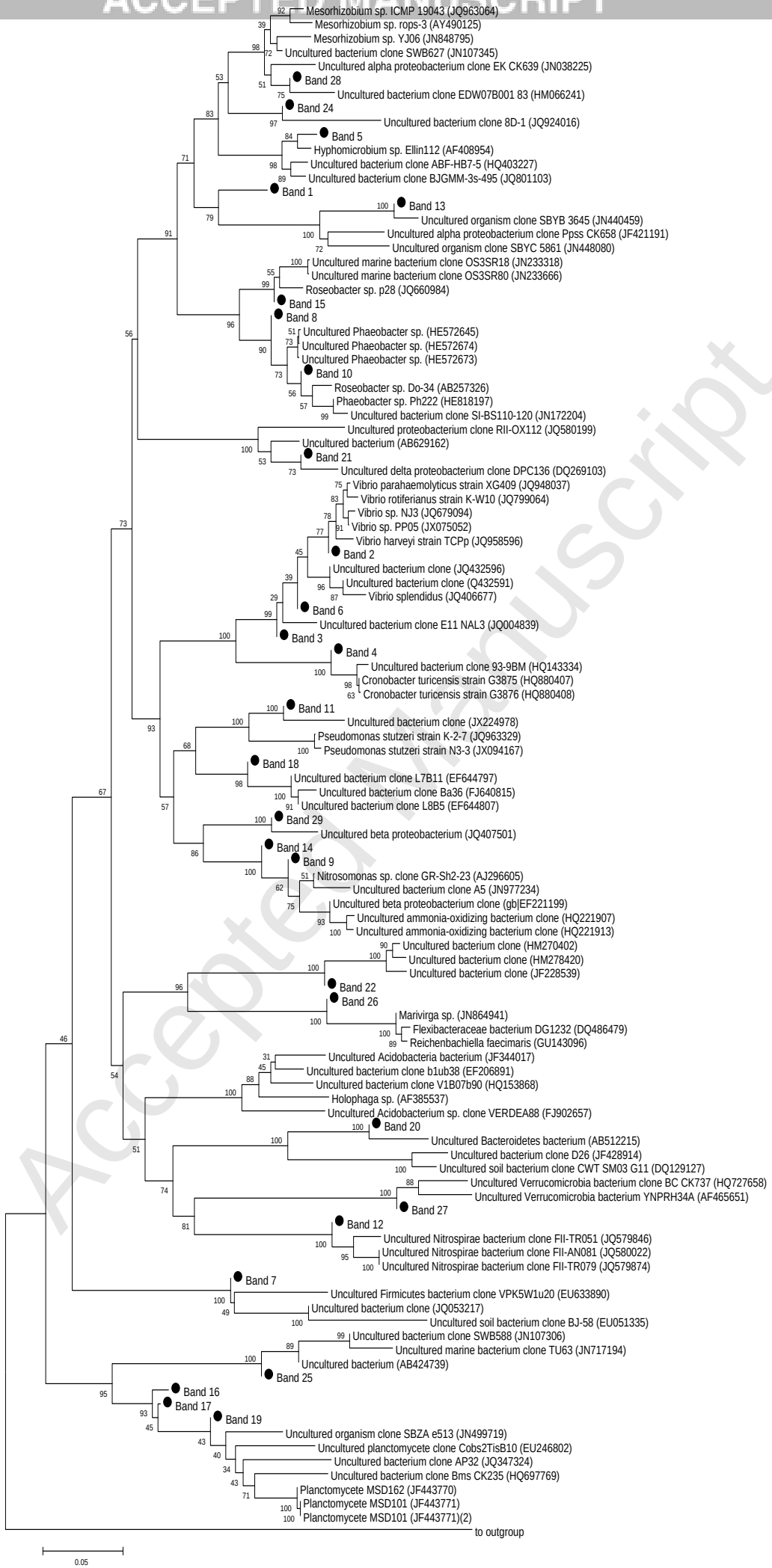


**FIG. 5:** Jukes-Cantor distance estimation algorithm showing affiliation of DGGE bands closest-related sequences. Percentages of 500 bootstrap resampling that supported the branching orders in each analysis are shown above or near the relevant nodes. The tree was out grouped with 16S rRNA gene sequence of Methanocaldococcus jannaschii DSM 2661

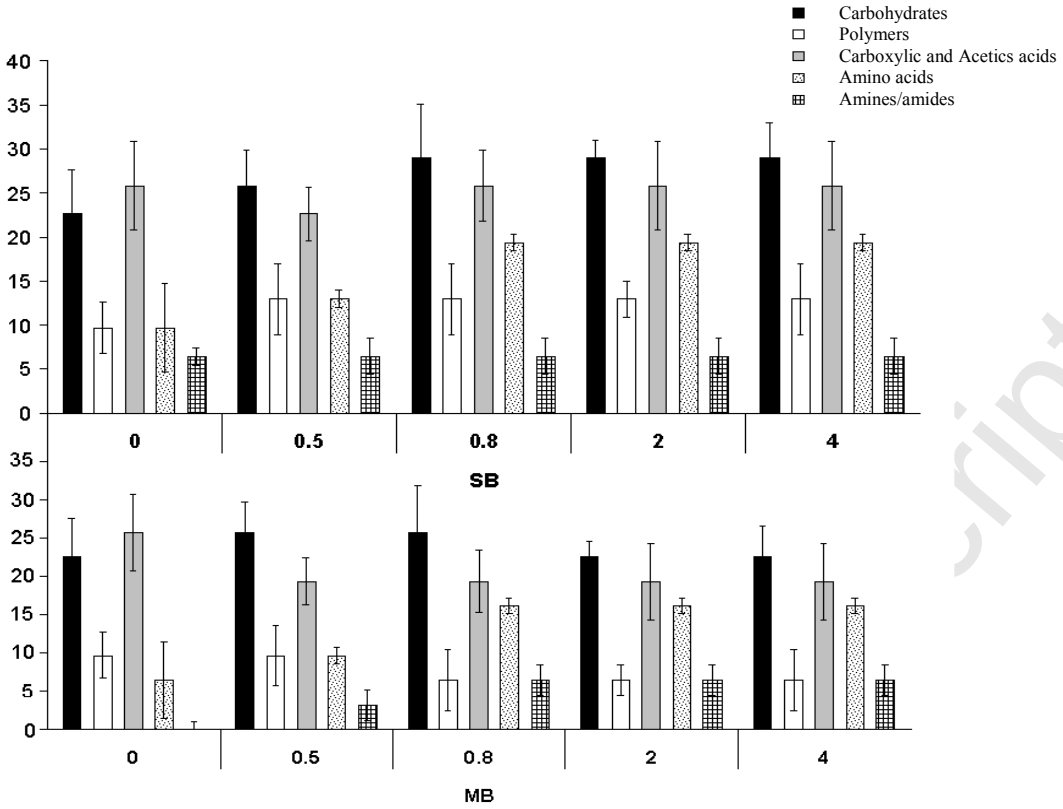


**Fig. 6 -** Percentage of total carbon source utilization at different C/N ratios for the different guilds. Carbohydrates (*Carb*), polymers (*Poly*), carboxylic and acetic acids (*C&AA*), amino acids (*AA*), amines and amides (*A&A*). SB, Static Bed Biofilter; MB, Moving Bed Biofilter.

**Table 1** - Oligonucleotide probes used in this study.

| Probe* | Specificity | Probe sequence (5'-3') | FA (%)† | Target site 16S or 23S rRNA position (nucleotide) | Reference |
|---|---|---|---|---|---|
| EUB338I | Most but not all *Bacteria* | GCTGCCTCCCGTAGGAGT | 0-35 | 16S (338-355) | Egli et al., 2003 |
| EUB338II | *Planctomycetes* | GCAGCCACCCGTAGGTGT | 0-35 | 16S (338-355) | Egli et al., 2003 |
| EUB338III | *Verrucomicrobiales* | GCTGCCACCCGTAGGTGT | 0-35 | 16S (338-355) | Egli et al., 2003 |
| NON-EUB | | ACTCCTACGGGAGGCAGC | 0-35 | 16S (338-355) | Manz et al., 1992 |
| ALF1b | *Alphaproteobacteria* | CGT TCGYTCTGAGCCAG | 20 | 16S (968-985) | Egli et al., 2003 |
| BET42a | *Betaproteobacteria* | GCCTTCCCACTTCGTTT | 35 | 23S (1027-1043) | Manz et al., 1992 |
| GAM42a | *Gammaproteobacteria* | GCCTTC CCACATCGTTT | 35 | 23S (1027-1043) | Manz et al., 1992 |
| DELTA495a | Most *Deltaproteobacteria* and most *Gemmatimonadetes* | AGTTAGCCGGTGCTTCCT | 35 | 16S (495 – 512) | Manz et al., 1992 |
| DELTA495b | some *Deltaproteobacteria* | AGTTAGCCGGCGCTTCCT | 35 | 16S (495 – 512) | Manz et al., 1992 |
| DELTA495c | some *Deltaproteobacteria* | AATTAGCCGGTGCTTCCT | 35 | 16S (495 – 512) | Manz et al., 1992 |
| EPSY549 | *Epsilonproteobacteria* | CAGTGATTCCGAGTAACG | 35 | 16S (549 – 566) | Manz et al., 1992 |
| PLA46 | *Planctomycetes* | GACTTGCATGCCTAATCC | 35 | 16S (886–904) | Neef et al., 1998 |
| CF319a | *Cytophaga-Flavobacterium* cluster | TGGTCCGTGTCTCAGTAC | 35 | 16S (319-336) | Manz et al., 1992 |
| HGC69a | *Actinobacteria* (high G+C content - Gram-positive bacteria) | TATAGTTTACCACCGCCGT | 25 | 23S (1901-1918) | Meier et al., 1999 |
| LGC354a | *Firmicutes* (low G+C content - Gram-positive bacteria) | TGGAAGATTCCCTACTGC | 35 | 16S (354-371) | Meier et al., 1999 |
| LGC354b | *Firmicutes* (low G+C content - Gram-positive bacteria) | CGGAAGATTCCCTACTGC | 35 | 16S (354-371) | Meier et al., 1999 |
| LGC354c | *Firmicutes* (low G+C content - Gram-positive bacteria) | CCGAAGATTCCCTACTGC | 35 | 16S (354-371) | Meier et al., 1999 |

* Probes EUB338I, EUB338II e EUB338III were equimolarly mixed together to obtain the EUB-mix; the probes DELTAa , DELTAb and DELTAc were equimolarly mixed together to obtain the DELTA-mix; the probes LGC354a, LGC354b e LGC354c were equimolarly mixed together to obtain the LGC-mix.

†: Values represent percent of formamide in the hybridization buffer.